45th Aerospace Sciences Meeting & Exhibit ***AIAA-2007-0087***
January 8-11, 2007 Reno, NV

Aerodynamic Simulation of a Horn-ice Accretion on a Subscale Model

Greg Busch,[*] Andy Broeren,[†] and Michael Bragg[‡]
University of Illinois at Urbana-Champaign, Urbana, IL 61801

The objective of this investigation was to determine the simulation fidelity required to accurately model the aerodynamics of a horn-ice ice accretion. Several simulations of differing fidelity, ranging from a low-fidelity, simple-geometric simulation to a high-fidelity, 3-D casting, were constructed to model a horn-ice accretion. The aerodynamic performance parameters C_l, C_m, and C_d and flow visualization images were obtained for each simulation and compared to those of the 3-D casting. Aerodynamic testing was performed in the University of Illinois 3 x 4 ft. subsonic wind tunnel at a Reynolds number of 1.8 million and a Mach number of 0.18. The results of the study showed that the horn-ice casting caused a 55% reduction in maximum lift and a 400% increase in minimum drag at this Re and M. The 2-D smooth simulation had a maximum lift coefficient within 0.2% of the casting, and was the simplest simulation to accurately model maximum lift. It under-estimated drag slightly, but fell within the uncertainty caused by the spanwise variation present in the flowfield of the casting. A higher fidelity simulation proved to have a slightly higher accuracy for modeling both lift and drag and the spanwise variation of the casting flowfield, but was substantially more difficult to construct. Therefore, the 2-D smooth simulation is recommended for most applications.

Nomenclature

α	airfoil angle of attack
c	airfoil chord length
C_d	drag coefficient
$C_{d,min}$	minimum drag coefficient
C_l	lift coefficient
$C_{l,max}$	maximum lift coefficient
C_m	quarter-chord pitching-moment coefficient
C_p	pressure coefficient
k	feature height
M	freestream Mach number
Re	freestream Reynolds number, based on the airfoil chord length
s	airfoil model coordinate along the surface length
SG	simple-geometric ice simulation
θ	ice-shape horn angle with respect to the chordline
x	coordinate in the airfoil model chordwise direction
y	coordinate normal to the airfoil model chordline
z	coordinate in the airfoil model spanwise direction

I. Introduction

To promote safety and reliability of operations, aircraft are certified for flight into icing conditions. Manufacturers can achieve this certification in part by demonstrating that their aircraft can fly safely after an ice accretion has formed. This is difficult to do in flight tests using a natural ice accretion, as it is hard to find a large

[*] Graduate Research Assistant, Department of Aerospace Engineering, Member AIAA.
[†] Research Scientist, Department of Aerospace Engineering, Senior Member AIAA.
[‡] Professor of Aerospace Engineering, Associate Dean for Research and Administrative Affairs, Fellow AIAA.

uniform icing cloud with the desired conditions. Therefore, simulations are often used to represent the ice accretion aerodynamically. These simulations can have a very high fidelity, capturing all of the three-dimensionality and roughness of the actual ice accretion, or they can be of lower fidelity, representing only the main features of the ice accretion using simple geometric shapes such as triangles or rectangles. High fidelity simulations are usually expensive and time consuming to produce, so it is often necessary to use a lower fidelity simulation. This paper investigates the effects of using simulations of varying fidelity to determine the aerodynamics of a horn-ice accretion and make recommendations as to the fidelity required to make an accurate horn-ice accretion simulation. This work was conducted as a part of a research program described in a companion paper by Bragg et al.[1] The overall program considers three other types of ice accretion in addition to the horn ice presented here. The overall program includes the use of computational methods as well as ice accretion and aerodynamic testing on a full-scale model.

The horn-ice accretions simulated in this study were of glaze ice, which typically forms at temperatures just below freezing when water droplets impinge on the airfoil, form a wet surface, and later freeze on the airfoil surface or on the ice shape itself. This may cause a horn to form on only the upper surface or on both the upper and lower surfaces. Because the water can flow on the surface before freezing, the stagnation point area is typically covered only by a thin, smooth layer of ice. Behind the horn is a region of highly three-dimensional ice feathers and nodules. Bragg, Broeren, and Blumenthal[2] have identified the key aerodynamic characteristics of a horn-ice accretion. A separation bubble forms behind the upper-surface horn as a result of the severe adverse pressure gradient at the tip of the horn. Since the separation point is relatively fixed at the tip of the horn, Reynolds number effects are generally small. The separation bubble, similar to the long bubble described by Tani,[3] dominates the airfoil aerodynamics. The size of this separation bubble is determined by the main geometric characteristics of the horn, such as horn height (k/c), horn location (s/c), horn angle (θ), and sometimes horn tip radius (r/c). Horn-ice accretions generally cause severe penalties to $C_{l,max}$ and induce thin-airfoil stall, as characterized by McCullough and Gault.[4]

Several methods can be used to generate simulations of horn-ice accretions. Taking a mold of the ice accretion and using it to construct a casting yields the highest fidelity simulation, known as a 3-D casting. This type of simulation captures nearly all of the three-dimensionality and detail of the original ice accretion. It is generally considered to give the true aerodynamics of the ice accretion, and can be used to determine the accuracy of results obtained from other types of simulations of the same accretion. Simpler simulations can be created by making a tracing of the ice accretion or casting and extruding it to form what is known as a 2-D smooth simulation. An even simpler representation may be obtained by using simple-geometric shapes, such as triangles or rectangles, that imitate the main features of the ice accretion. Neither the 2-D smooth nor simple-geometric simulations capture spanwise variation of the ice accretion, but they can be manufactured quickly and inexpensively. This makes them ideal simulations for use in parametric studies, such as that of Kim and Bragg,[5] Lee,[6] and Papadakis et al.[7] Other types of simulations include 2-D smooth or simple-geometric simulations with either non-periodic or periodic spanwise variation. These simulations capture the spanwise variation of the important geometric features of the ice shape, but do not model the highly three-dimensional features such as ice feathers or nodules. Additionally, surface roughness may be added to change the fidelity of any of these simulations.

The level of smoothing used to create 2-D smooth simulations may also be important. Smoothing of the 2-D smooth shape refers to the removal of small irregularities in the shape that occur due to the tracing of surface roughness. Extending this local 3-D roughness spanwise is inappropriate and thus a smoothing process is often used to remove these features. If a simulation is generated by making a tracing of the ice accretion, a small level of smoothing results. To achieve a higher level of smoothing, the ice shape tracing is digitized and the computer program SmaggIce[8] can be used to remove a certain percentage of control points.

Several studies have already been conducted comparing the results of one type of horn-ice shape simulation to another. Gurbacki compared a 3-D casting of a horn-ice accretion on a NACA 0012 to a 2-D smooth simulation of the same accretion which used 50% control points.[9] It was found that the 3-D casting had a higher $C_{l,\,max}$ and a shorter separation bubble than the 2-D smooth simulation. However, other tests comparing a 3-D casting to a 2-D smooth simulation have had different results. Addy and Chung investigated a horn-ice shape on an NLF-0414 airfoil.[10] For this study, the 2-D smooth simulation, which used 30% control points, had a higher $C_{l,\,max}$ than the 3-D casting. This suggests that some of the features present on the 3-D casting and not represented by the 2-D smooth simulation have an effect on the airfoil aerodynamics. In another comparison between a 3-D casting and a 2-D smooth horn-ice simulation performed by Addy et al.,[11] both simulations had the same penalty to $C_{l,\,max}$. This study, performed on an airfoil similar to the GLC-305, used 100% control points to create the 2-D smooth simulation. Blumenthal et al.[12] attempted to address these discrepancies by performing a parametric study on a horn-ice simulation on a NACA 0012. The geometry of the upper- and lower-surface horns was varied to reflect tracings

taken at different spanwise locations. This study showed that small changes in the upper-surface horn geometry that may result from different tracing locations have an effect on the airfoil $C_{l\,max}$ that is comparable in magnitude to the differences seen in the studies comparing 3-D castings to 2-D smooth simulations. Therefore, if the tracing is taken at a location that is unrepresentative of the mean effective horn height of the casting, the 2-D smooth simulation will have a different mean effective horn height and will likely have a different $C_{l,\,max}$.

Other studies provide conflicting results as to what level of detail is required for a simulation to represent an ice accretion aerodynamically. For example, Kim and Bragg parametrically varied the horn height, angle, and tip radius of a simple geometric horn-ice simulation on a NLF-0414 airfoil. Changes in the tip radius had virtually no effect on $C_{l,max}$. In another study on a 2-D smooth simulation of a horn-ice shape on a NACA 0012 airfoil, a decrease in the tip radius of the upper-surface horn caused a decrease in $C_{l,max}$ of 8%. These contrasting results may be due to differences in the airfoils used. The NACA 0012 has a large suction peak near its leading edge and is highly sensitive to the presence of an ice shape, whereas the NLF-0414 is more uniformly loaded and is less sensitive to leading-edge ice accretion.

The effect of surface roughness on a horn-ice simulation is also unclear. In one fluorescent oil-flow visualization study, it was found that adding roughness to a 2-D smooth ice shape generated cell structures similar to those seen on the 3-D casting and caused the separation bubble reattachment line to move approximately 5-10% farther upstream.[13] No performance data were taken in this study, so the effect of the roughness elements on $C_{l,\,max}$ was not determined. Another study by Addy et al.[11] found that the addition of 30-grit roughness had no effect on the airfoil $C_{l\,max}$ and only a minor effect on C_d. The authors pointed out that different methods of applying roughness may give different results. For example, there are no standardized methods for determining the appropriate roughness size and concentration, and there are different interpretations of what type of roughness will give the best representation of an ice accretion.

The main objective of this study was to determine the level of simulation detail required to aerodynamically represent a horn-ice accretion. To construct the simulations, a 3-D casting was created from ice accreted in an icing tunnel. This casting was traced and measured to generate 2-D and 3-D simulations of varying fidelity. The aerodynamic performance of these simulations was then compared to that of the 3-D casting. All aerodynamic testing was performed in the University of Illinois 3 x 4 ft. subsonic wind tunnel at Re = 1.8×10^6 and M = 0.18 on an 18-inch chord NACA 23012 airfoil model.

II. Experimental Methods

The aerodynamic testing in this study was conducted in the University of Illinois subsonic, low-turbulence, open-return wind tunnel, which had a test section measuring 2.8 ft. high, 4 ft. wide, and 8 ft. long. The test section widened approximately 0.5 inches over its length to account for growth in the wall boundary layer. The inlet contraction ratio of the tunnel was 7.5:1. A four-inch honeycomb and four anti-turbulence screens were used to reduce the empty test-section turbulence intensity to less than 0.1% at all operating speeds for a bandwidth of 10-5000 Hz.[14]

The aluminum NACA 23012 airfoil model used in this study, which had a chord of 18 inches and a span of 33.563 inches, had a removable leading edge to facilitate simple installation of ice accretion simulations. It had two chordwise rows of taps, a primary row and a secondary row. The primary row, located at 51% span, contained 43 taps. This spanwise location will be referred to as z = 0 inches in the discussion of results. The secondary row, located at 42% span, contained 22 taps. Additionally, the model had a row of spanwise taps on the upper surface, located at 70% chord. The layout of these taps made it possible to check for spanwise variation in the flow behind the ice shapes. The airfoil model is described in more detail by Blumenthal.[15]

Fig. 1 Traversable wake rake installed behind NACA 23012 model.

Lift and pitching moment coefficient data were obtained using both a three-component force balance and by integrating the measured surface pressures around the airfoil model. The drag coefficient was computed using data collected by a traversable wake rake which measured the static and total wake pressures. The experimental setup of the airfoil model and wake rake is shown in Fig. 1. An electronically scanned pressure system was used to measure the model surface and wake pressures. Blumenthal and Busch[16] describe the experimental setup in more detail. In this study,

model surface pressure measurements were used to obtain lift and pitching moment data, and the pressures measured by the wake rake were used to obtain the drag coefficient using standard momentum-deficit methods. The experimental uncertainties were calculated using the methods of Kline and McClintock[17] and Coleman and Steel,[18] and a summary of these uncertainties is given in Table 1. All testing was conducted at Re = 1.8×10^6 and M = 0.18.

Table 1 Sample uncertainties based on 3-D casting of horn-ice accretion at α = 4 deg. and Re = 1.8×10^6.

Parameter	Reference Value	Absolute Uncertainty	Relative Uncertainty (%)
α	4.163	± 0.02 deg.	± 0.480
C_l	0.502	± 0.000832	± 0.166
C_d	0.0459	± 0.000415	± 0.904
C_m	0.0335	± 0.000255	± 0.761
C_p	-1.263	± 0.0116	± 0.922

Fluorescent oil-flow visualization studies were also performed on selected simulations. For these studies, the airfoil model was coated with fluorescent oil that responded to the surface shear stress. Regions of high shear caused more oil movement than regions of low shear, so these regions do not appear to be as bright as the low shear stress regions. Using this technique, the flowfield can be examined to identify time-averaged separation bubble reattachment zones as well as regions of separation and reverse flow. The time-averaged separation bubble reattachment line can be estimated to within approximately $x/c = \pm 0.04$ using this method.

Bragg et al. describe the testing that yielded the horn-ice accretion investigated in this paper (Fig. 2). Several different simulations of varying fidelities were used to model the aerodynamics of this accretion. The highest fidelity simulation was a 3-D casting (Fig. 3a), which captures all of the three-dimensionality of the original ice accretion and is the most representative simulation. Pressure taps were installed directly in the casting, as it was shown in an earlier study that this yields results virtually identical to those obtained using a pressure slice.[12, 15]

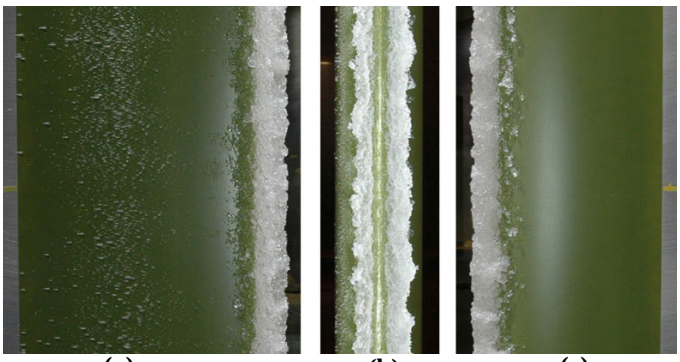

(a) (b) (c)

Fig. 2 Photographs of the original horn-ice accretion: (a) lower surface, (b) leading edge, and (c) upper surface of the airfoil.

The other simulations investigated were manufactured using rapid prototyping techniques. One of these was a simple-geometric simulation with non-periodic spanwise variation. This simulation was designed based on measurements of the upper and lower-surface horns on the casting. The height and angle of these horns were measured every 0.1 inches along the 11.187-inch span of the casting. Rectangles were then used to model the horn height and angle on the non-periodic simple-geometric simulation. The orientation of these rectangles varied every 0.1 inches along the span of the simulation so that the simulation horn height and angle would be representative of the casting. The simple geometric simulation with non-periodic spanwise variation is shown in Fig. 3b.

Other types of simulations tested were simple-geometric simulations with a uniform periodic variation of the horn height only. A statistical analysis was performed on the spanwise measurements discussed above to determine the average and RMS horn height and angle. The average horn height was $k/c = 0.047$ for the upper horn and $k/c = 0.032$ for the lower horn. The RMS horn height was $k/c = 0.0032$ and $k/c = 0.0028$ for the upper- and lower-surface horns, respectively. A 4096-point Fast Fourier Transform analysis was also performed on the spanwise measurements, and it was determined that the dominant period was 1.6 inches. Two simulations with uniform periodic variations were made, one with a period of 1.6 inches (Fig. 3c) and one with a period of 0.8 inches. The amplitude of the height variations for both of these simulations was one standard deviation.

The remaining simulations had a constant cross-section. One of these simulations was generated by making a tracing of the casting at the spanwise station at which the taps were located and extruding it over the span of the model. No additional smoothing, other than that which resulted from the tracing of the casting, was used. This 2-D simulation will be referred to as the 2-D smooth simulation (Fig. 3d). The final simulation was created by emulating the horn using simple-geometric shapes (rectangles). The cross-sections of these two simulations are shown in Fig.

4. Since the span of each of the simulations was only 11.187 inches and the airfoil model was 33.563 inches, three identical simulations of each type were constructed and placed end-to-end to form a 33.563-inch long ice shape.

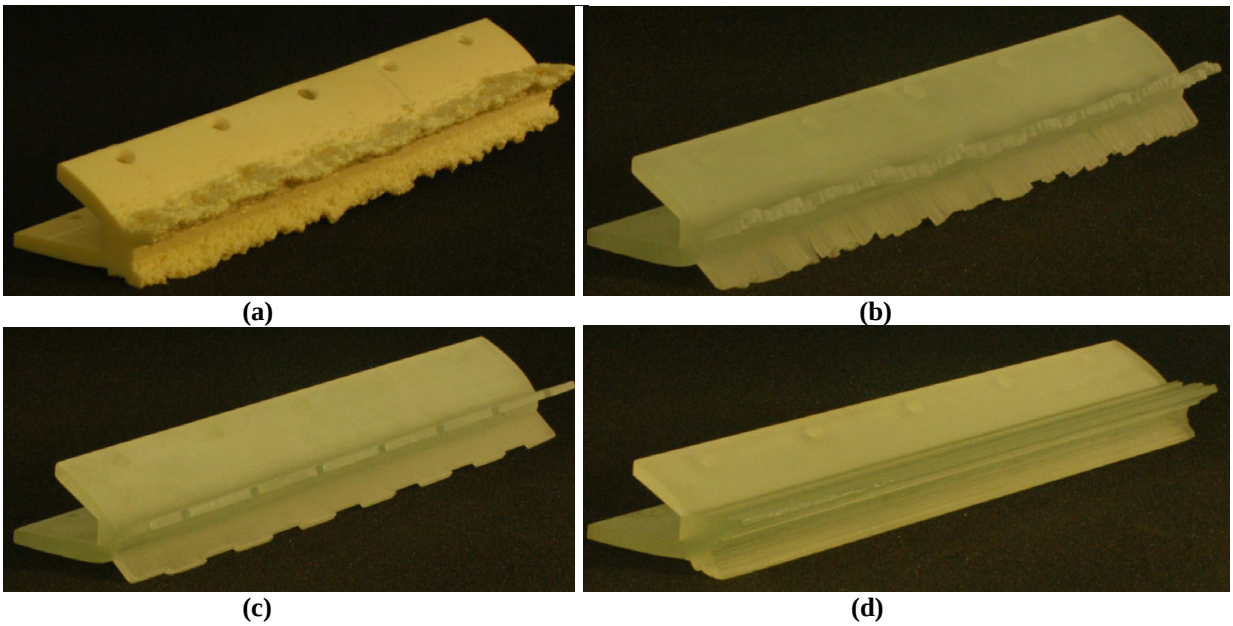

Fig. 3. Simulations of a horn-ice accretion: (a) 3-D casting, (b) simple geometric with non-periodic spanwise variation, (c) simple geometric with periodic spanwise variation, and (d) 2-D smooth simulations.

Finally, roughness elements of various sizes were added to each of the simulations (except the casting) to model the roughness of the ice accretion. Two different types of roughness elements were used: 14 grit silicon carbide and size 35 and 40 glass microbeads. Based on measurements of individual particles, these roughness elements had heights of k/c = 0.0033 and k/c = 0.0009, respectively. The silicon carbide roughness elements were irregularly shaped and jagged, whereas the glass microbeads were spherical. The addition of these roughness elements added a small-scale three-dimensionality to each of the simulations.

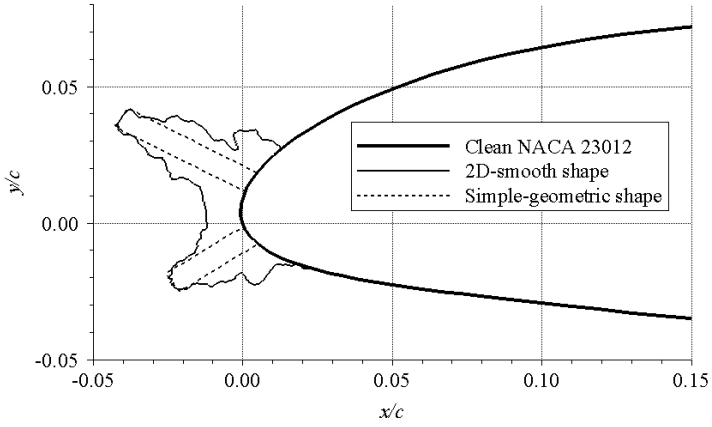

Fig. 4 Cross-sections of the 2-D smooth and simple-geometric simulations of the horn-ice accretion.

III. Results and Discussion

This section is divided into three subsections where the aerodynamic data are presented: 3-D casting, 2-D simulations and 3-D simulations. The 3-D casting captures nearly all of the geometric detail present in the original ice accretion and is assumed to be a true geometric and aerodynamic representation of the accretion. The 2-D simulations are those which were manufactured based on only a single spanwise measurement or tracing of the original accretion. These include a 2-D smooth simulation, which is an extrusion of a tracing of the accretion, and a simple-geometric simulation, which uses rectangles to model the upper and lower-surface horn height, location, and angle. The 3-D simulations required more detailed measurements to construct. These include two simple-geometric simulations with periodic spanwise variation of the upper and lower-surface horn height (with periods of 0.8 and 1.6 inches), and a simple-geometric simulation which varies both horn height and angle every 0.1 inches along the span based on measurements of the casting. Recall that the objective of this study was to determine the simulation fidelity required to accurately model the aerodynamics of the original horn-ice accretion.

A. 3-D Casting

The effects of the 3-D casting on the lift, pitching moment, and drag coefficients of the NACA 23012 are shown in Fig. 5. The clean airfoil had a $C_{l,max}$ of 1.48 at α = 14.4 deg. and a $C_{d,min}$ of 0.0070 at α = 0 deg. The addition of the 3-D casting caused a 55% reduction in $C_{l,max}$ and a 400% increase in $C_{d,min}$. It also caused the airfoil to switch from a leading-edge stall at α = 14.4 deg. to a thin-airfoil stall at α = 7.2 deg. The severe adverse pressure gradient generated by the horn caused a separation bubble to form, which can be seen in the flow visualization image of the casting taken at α = 4 deg. (Fig. 6a). In the image, flow is from left to right, and the 3-D casting is visible on the left. The horizontal scales at the top and bottom of the picture correspond to the chordwise station in percent chord, while the vertical scale on the right measures the spanwise station in inches. The reattachment zone of the separation bubble ranges from x/c = 0.15 near the top of the model to x/c = 0.20 near the bottom of the model. Inside of the separation bubble is a region of reverse flow, indicated by the oil streaks flowing from right to left. In addition to the separation bubble, the casting causes the formation of three-dimensional cell structures, similar to those seen in the studies of Gurbacki and Bragg and Blumenthal. As α increases to 5 deg. (Fig. 6b), the separation bubble reattachment zone moves downstream and ranges from x/c = 0.25 to 0.30 and the cell structures become larger and more clearly defined.

B. 2-D Simulations

Two 2-D simulations were tested: a 2-D smooth simulation and a simple-geometric simulation. The 2-D smooth simulation had a $C_{l,max}$ identical to that of the casting at the same stall angle of attack ($C_{l,max}$ = 0.66, α_{stall} = 7.2 deg.) and the simple-geometric simulation had a 2% lower $C_{l,max}$ of 0.65 (Fig. 5a). The stall type of each of the 2-D simulations was thin-airfoil stall, as was that for the 3-D casting. Both simulations had a higher C_m than the casting at all positive angles of attack well-below stall, but were within 5% at α = 5 deg., the angle after which C_m began to decrease due to the initial onset of stall. Beyond α = 5 deg., the 2-D simulations both under-predicted C_m.

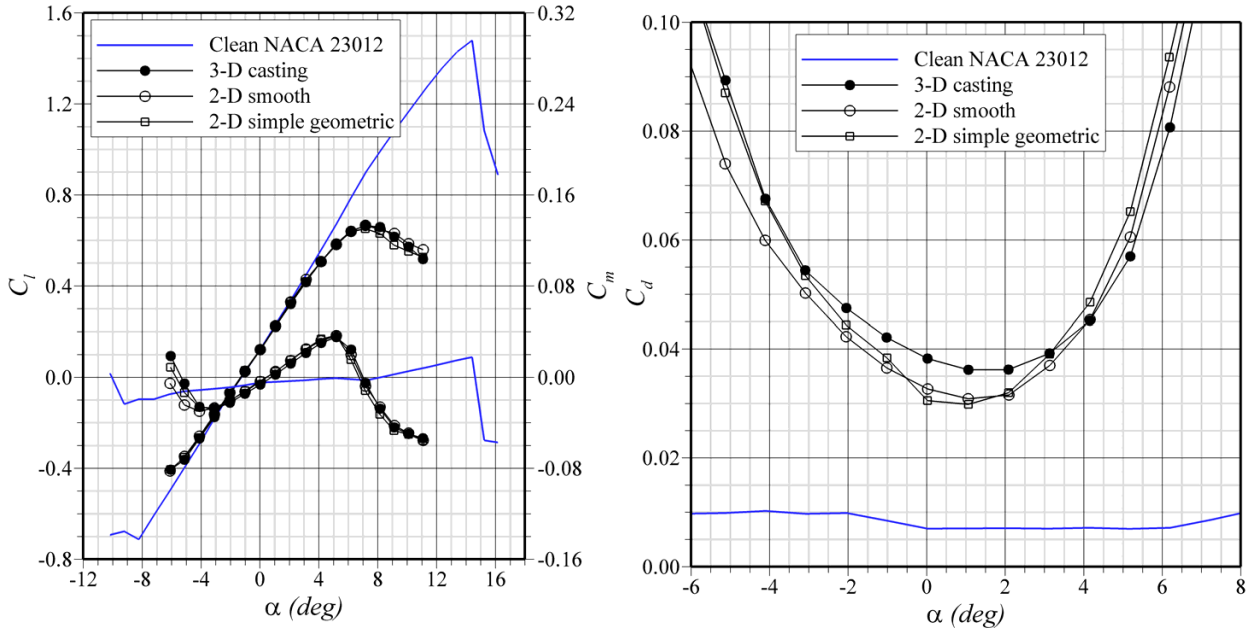

Fig. 5 Comparison of (a) C_l and C_m and (b) C_d between the 3-D casting and each 2-D simulation at Re = 1.8 million and M = 0.18.

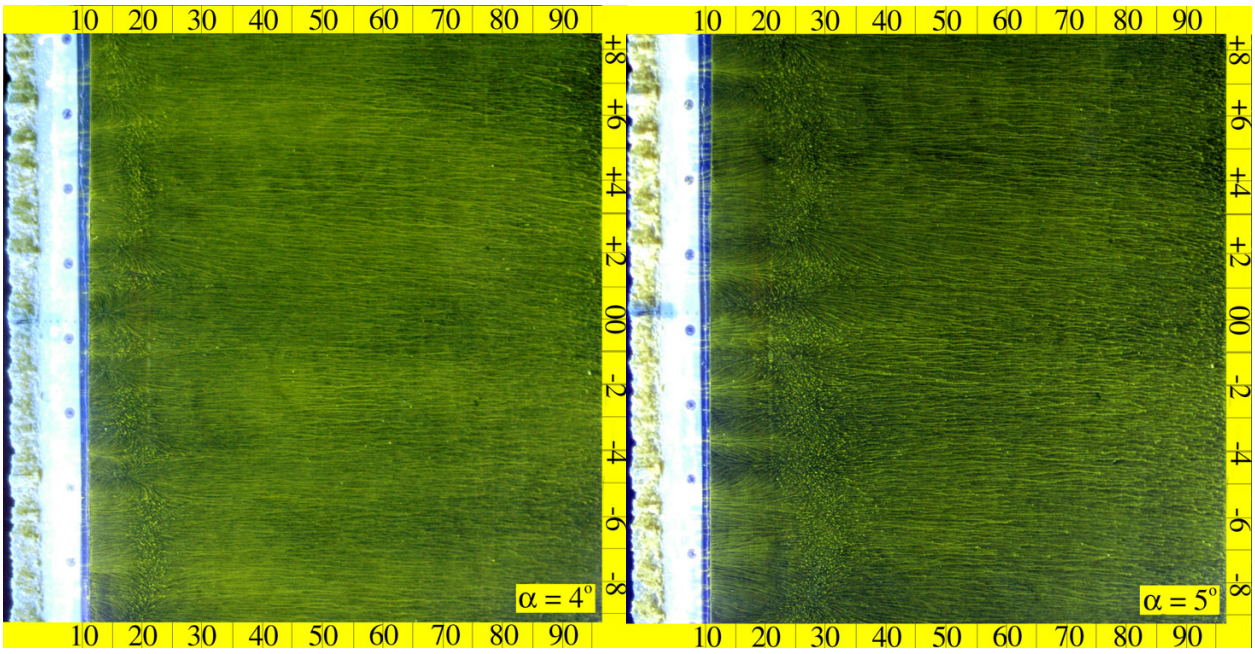

(a) **(b)**

Fig. 6 Fluorescent oil-flow visualization of 3-D casting at (a) α = 4 deg. and (b) α = 5 deg. at Re = 1.8 million. Flow is from left to right.

The pressure distribution of Fig. 7 shows a slightly larger constant pressure plateau at α = 5 deg. for the simple-geometric simulation than for the other two simulations, indicating that it had a slightly larger separation bubble. This likely contributed to its lower $C_{l,max}$. This difference in separation bubble size can also be seen in the flow visualization image of the simple-geometric simulation, shown in Fig. 8a. The separation bubble reattachment zone ranged from approximately x/c = 0.32 to 0.38 for the simple-geometric simulation at α = 5 deg., approximately 8% farther downstream than was the case for the casting. The separation bubble of the 2-D smooth simulation reattached between x/c = 0.28 and x/c = 0.35 at the same angle of attack (Fig. 8b), and was therefore approximately the same size as the separation bubble of the casting (within the experimental uncertainty of x/c = ±0.04). Unlike in the case of the casting, no three-dimensional cell structures were observed in the flowfield of either 2-D simulation.

The comparison of the C_d curves of the 3-D casting and the 2-D simulations is shown in Fig. 5b. At low angles of attack, C_d of both of the 2-D simulations was well below that of the casting. As α increased, C_d of the 2-D simulations increased more rapidly than C_d of the casting, causing them to over-predict C_d at higher angles. This resulted in an RMS difference in C_d of 0.0062 between the 3-D casting and the simple-geometric simulation and of 0.0054 between the 3-D casting and the 2-D smooth simulation (from α = -4 deg. to 6 deg.). The higher C_d of the 3-D casting from α = -2 deg. to 2 deg. may be due to

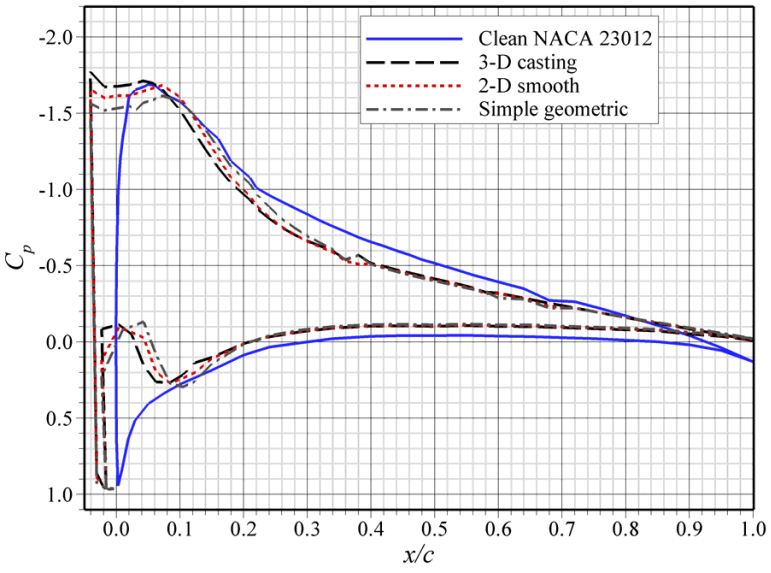

Fig. 7 Comparison of C_p between 3-D casting and 2-D simulations at α = 5 deg. and Re = 1.8 million.

the rough surface of the casting. Since no roughness was present on either of the 2-D simulations, they were unable to accurately model C_d over this α range.

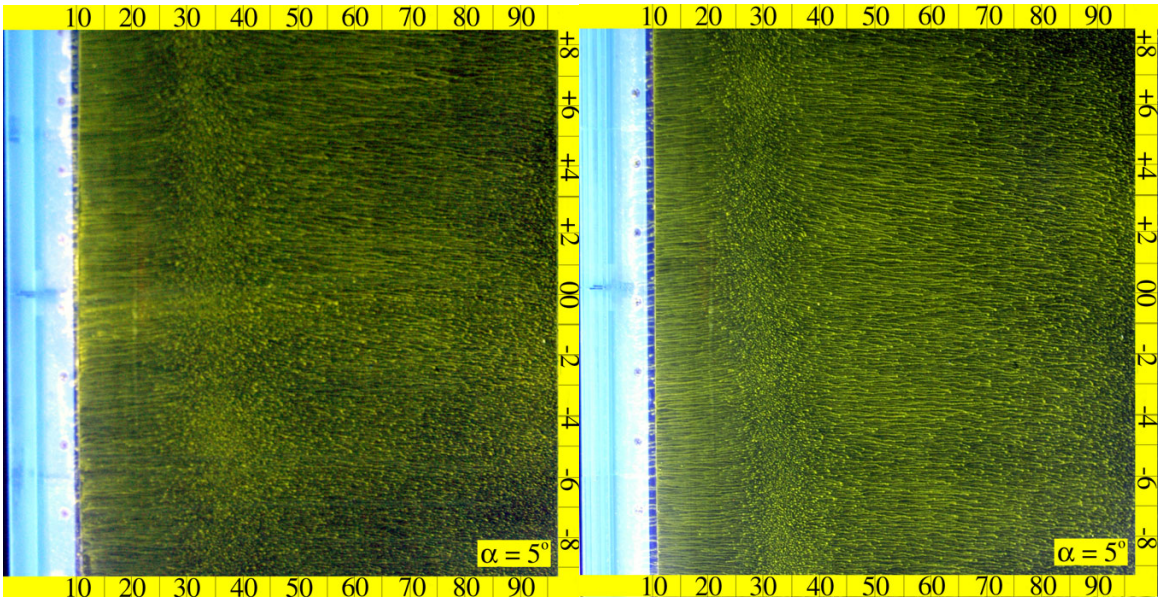

(a) **(b)**

Fig. 8 Flow visualization images of (a) simple-geometric and (b) 2-D smooth horn-ice simulations at α = 5 deg. and Re = 1.8 million.

To investigate these roughness effects, two different types of roughness were added to each of the 2-D simulations: size 35 and 40 microbeads, with a height k/c = 0.0009 and a concentration of 80%, and 14 grit silicon carbide, with a height k/c = 0.0033 and a concentration of 50%. The effect of these roughness elements on C_d are shown in Fig. 9. As a result of this roughness, the C_d curve was shifted upwards, causing both the simple-geometric and the 2-D smooth simulation C_d to more closely match the casting C_d at low angles of attack but causing each of them to have a much higher C_d at high angles of attack. When size 35 and 40 microbeads were added to the simple-geometric simulation, the RMS difference decreased to 0.0052 (relative to the 3-D casting), better than for either simulation without roughness. However, in every other case, the RMS difference in C_d increased. Additionally, the roughness present on the casting was much larger than the size 35 and 40 microbeads, illustrating that it would be very difficult to determine the roughness size that would most accurately simulate the accretion aerodynamics without advance knowledge of these aerodynamics.

Roughness also had a minor affect on C_l, as shown in Fig. 10. The larger 14 grit roughness size (k/c = 0.0033) caused penalties to $C_{l,max}$ of 8% and 7% for the simple-geometric and 2-D smooth simulations, respectively. Papadakis et al.[19] also investigated the effects of surface roughness on a horn-ice accretion. In that study, horn-ice shapes were generated by the NASA Glenn LEWICE 2.0 ice accretion code[20] for a swept wing using a GLC-305 airfoil, and the aerodynamic penalties both with and without the addition of 36 grit roughness (k/c = 0.0011) were measured. As in the present study, it was found that the addition of roughness tended to increase the aerodynamic penalties associated with the ice accretion simulations. In another study by Papadakis et al.,[21] 24 grit roughness (k/c = 0.0012) was added to LEWICE shapes generated for a 24-inch chord 2-D model of the horizontal tail of a DeHavilland DHC-6 Twin Otter aircraft. Again, the addition of roughness was found to decrease $C_{l,max}$ and increase C_d.

Flow visualization of the 2-D smooth simulation with 14 grit roughness at α = 5 deg. is shown in Fig. 11. The separation bubble is longer than it was for the 2-D smooth simulation without additional roughness, not reattaching until approximately x/c = 0.45 to 0.50. This is consistent with the observed effects on C_l and C_d. Also, the flowfield has little spanwise variation, as it did before roughness was added. This contrasts with the study of Jacobs, in which the addition of roughness caused cell structures to form similar to those seen in the flowfield of the casting. Since the $C_{l,max}$ of these simulations agreed with the casting before roughness was added, 14 grit roughness served only to decrease the simulation accuracy. The size 35 and 40 microbeads had a smaller effect, with virtually no difference measured for $C_{l,max}$ of the simple-geometric simulation and only a 3% decrease for the 2-D smooth simulation. This

caused the 2-D smooth simulation with size 35 and 40 microbeads to underestimate $C_{l,max}$ of the casting by 3%. Therefore, roughness, while noticeably affecting C_d, did not seem to significantly increase simulation fidelity in a predictable fashion when added in a uniform manner. One way to more accurately predict C_d might be to strategically size and position the roughness around the ice simulation to better tailor the drag performance versus angle of attack.

Given that the 2-D smooth and simple-geometric simulations were of similar manufacturing difficulties and that the 2-D smooth simulation gave a slightly more accurate estimate of both $C_{l,max}$ and C_d, it appears as if the 2-D smooth simulation is a better choice than the simple-geometric simulation at this time. However, both simulations gave accurate estimates of $C_{l,max}$, indicating that each appropriately represented the most important ice-shape features that determine this parameter. These features are the horn surface location, horn height, and horn angle. Neither of these simulations appears to have provided accurate estimates of C_d, and this will be discussed further in the next section.

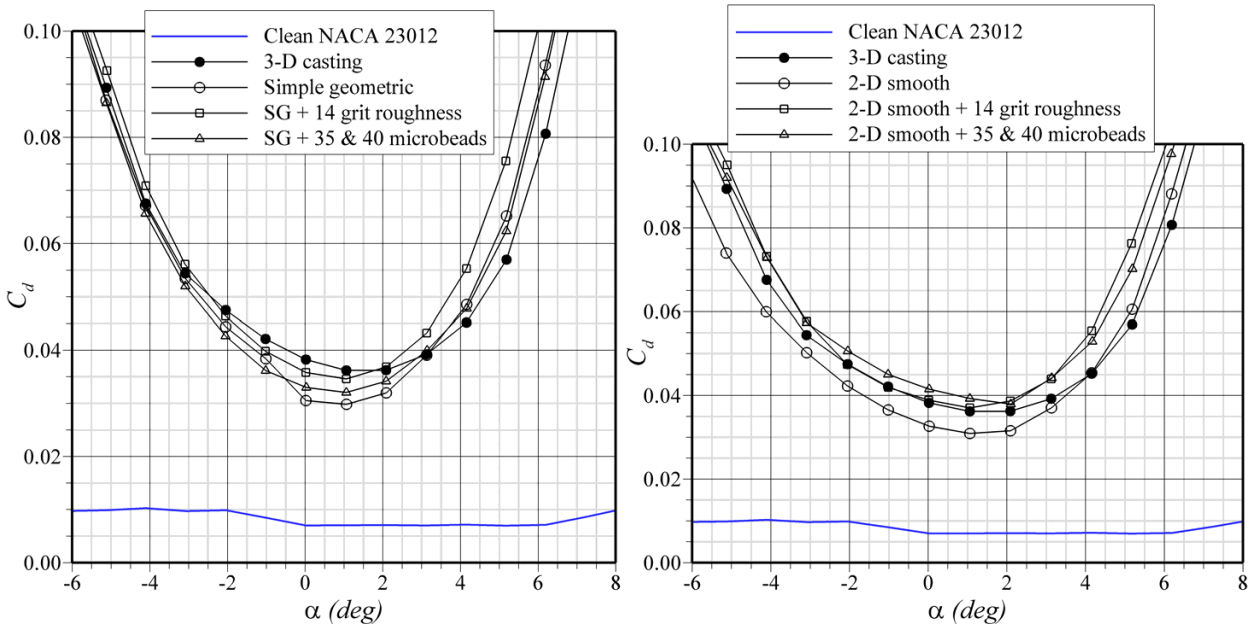

Fig. 9 Effect of surface roughness on C_d of the (a) simple-geometric and (b) 2-D smooth horn-ice simulations at Re =1.8 million.

C. 3-D Simulations

Recall that three simple-geometric simulations with spanwise variation were also tested. Two of these simulations varied the horn height periodically (with periods of 0.8 and 1.6 inches) and the third varied both the horn height and angle in a non-periodic manner so as to match the spanwise variation of the 3-D casting (this simulation will be referred to as the non-periodic simulation). These simulations are shown in Fig. 3. The aerodynamic penalties due to each are compared with those of the casting in Fig. 12. The 0.8-inch period simulation under-predicted $C_{l,max}$ by 4%. The 1.6-inch period simulation had an even lower $C_{l,max}$ (7% lower than the casting) but stalled 1 deg. later than any of the other simulations. This difference in $C_{l,max}$ was despite the fact that both of the periodic simulations had the same average horn height as the 2-D simple-geometric simulation. Unlike the periodic simulations, the non-periodic simulation had the same $C_{l,max}$ as the casting. Like the 2-D simulations, every 3-D simulation overestimated C_m at positive angles of attack before stall.

The ability of the 3-D simulations to model C_d of the casting is shown in Fig. 12b. The C_d curves of the two periodic simulations were very similar to each other, but are shifted by about 2 deg. compared to the C_d curve of the casting. Each of these simulations also had a $C_{d,min}$ approximately 10% lower than that of the casting.

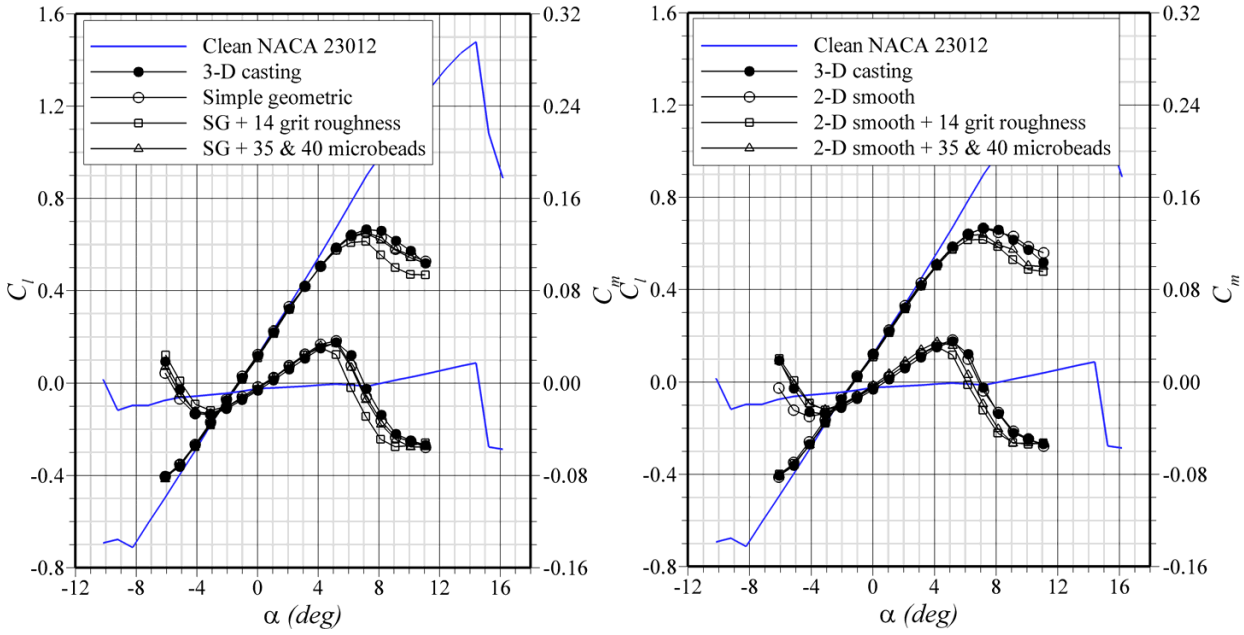

Fig. 10 Effect of surface roughness on C_l and C_m of the (a) simple-geometric and (b) 2-D smooth horn-ice simulations at Re =1.8 million.

Surface roughness was added to each of the 3-D simulations in an attempt to improve their ability to estimate C_d. The 0.8-inch and 1.6-inch period simulations with roughness were similar in their ability to model the drag performance of the 3-D casting. The additional roughness had effects similar to those seen with the simple-geometric shapes in Figs. 9a and 10a, in general causing a decrease in $C_{l,max}$ and an increase in C_d. Overall, roughness did not improve the modeling of either of these parameters. Additional details can be found in Busch.

The non-periodic simulation, on the other hand, greatly improved the simulation of C_d at all angles of attack (Fig. 12b). The RMS difference in C_d between the casting and the non-periodic simulation was only 0.0021 from α = -4 deg. to 6 deg. This may have been caused by the irregularities of the simulation due to the frequent change in cross-section geometry (in contrast to adding roughness or regular spanwise variation). This may provide a key to improving the simulation of C_d in the future.

Flow visualization images for the non-periodic simulation reveal three-dimensional cell structures nearly identical to those seen with the 3-D casting (Fig. 13). Both the size and spacing of the cells is similar and they are located at the same spanwise stations. In the figure, the curve illustrates the approximate mean separation bubble reattachment line, and it is clear that the reattachment line varies in the same manner for both the casting and the non-periodic simulation. The 1.6-inch periodic simulation also demonstrated the cell structures (Fig. 14a), but the cells did not accurately replicate those of the 3-D casting. The spacing was determined by the period of the simulation and the spanwise location of the cells corresponded to areas of low horn height. No cells were clearly visible in the flow visualization of the 0.8-inch period simulation at α = 5 deg. (Fig. 14b), but the flow

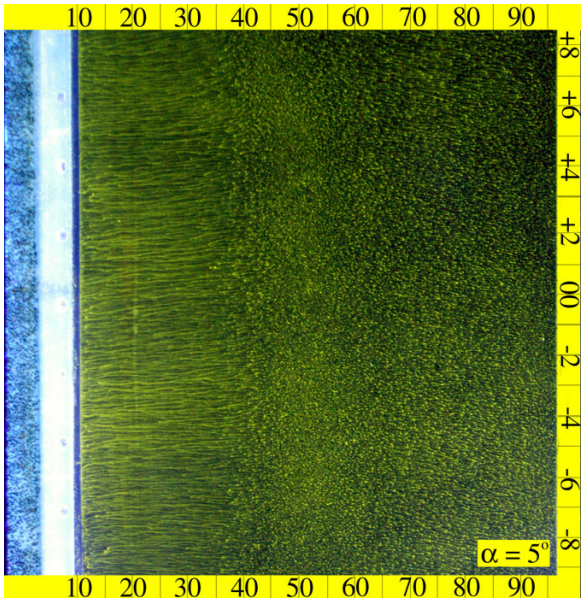

Fig. 11 Fluorescent oil-flow visualization of 2-D smooth simulation with 14 grit roughness at α = 5 deg. and Re = 1.8 million.

visualization at α = 4 deg. showed some cell structures that weren't well-defined. The cell structures were sufficiently close together that they merged at the higher angle of attack. Neither of the periodic simulations nor the 2-D smooth simulations (with or without roughness) had as much spanwise variation in the reattachment zone location as did the 3-D casting and the non-periodic simulation, suggesting that non-periodic variation of the horn geometry is necessary to accurately model this feature of the separation bubble behind the horn.

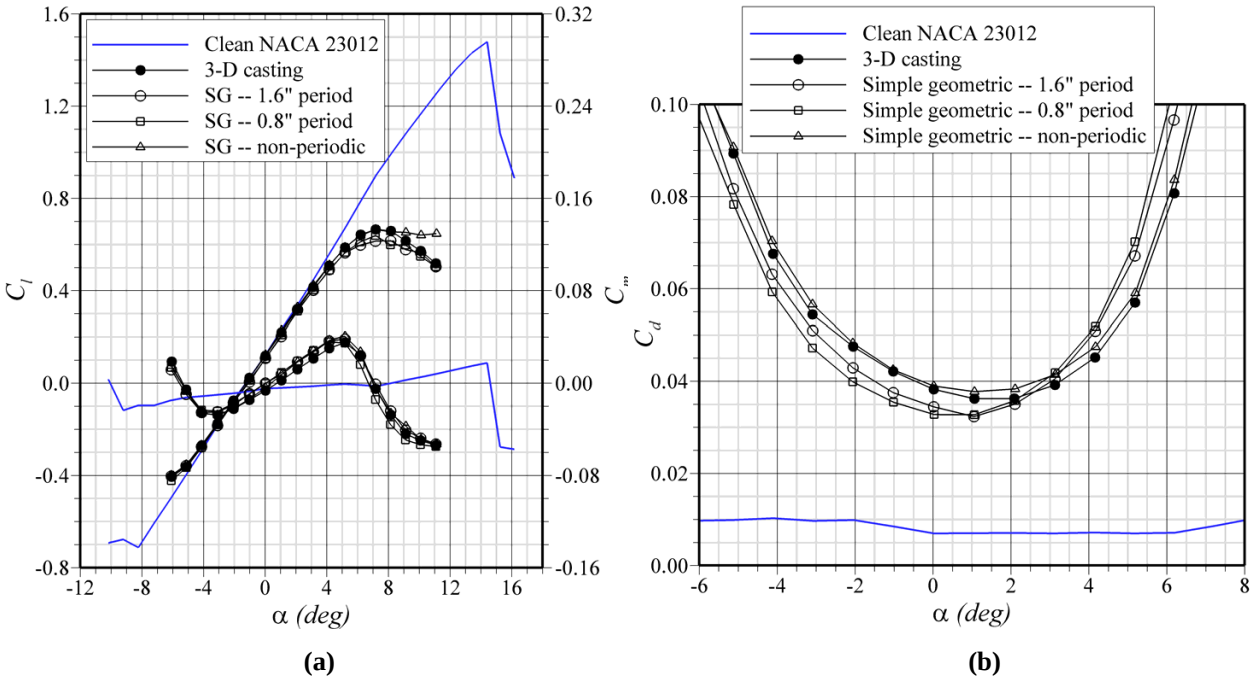

Fig. 12 Comparison of (a) C_l and C_m and (b) C_d between the 3-D casting and each 3-D simulation at Re = 1.8 million.

The C_p distributions for each of the 3-D simulations are shown in Fig. 15. The non-periodic simulation had the C_p distribution that was closest to the casting. Both of the simple-geometric simulations with periodic spanwise variation had trailing-edge pressures that were slightly higher than that of either the casting or non-periodic simulations. Additionally, the magnitude of the constant pressure plateau beginning at x/c = -0.04 was less for the periodic simulations, contributing to lower lift coefficients.

All of the measurements of C_d discussed previously were taken at a spanwise location of z = 3.63 inches. However, flow visualization revealed that there was significant spanwise variation in the flowfield of the 3-D casting, so several measurements of C_d were taken to provide a more comprehensive comparison with the casting. To make this comparison, C_d was measured every half inch along the span over the center 7.5 inches of the model for several of the simulations. An additional measurement was taken at z = 3.63 inches. The data were taken in four angle of attack sweeps, during each of which C_d was measured at 6 spanwise stations. The data from z = 0 to 3.0 inches was measured twice to ensure repeatability. C_d was therefore measured in a total of 17 different spanwise planes. The spanwise variation in C_d of the 2-D simulations are shown in Fig. 16a. The simple-geometric simulation had no spanwise variation, so ideally it would have had the same C_d at each spanwise station. At α = 4 deg., this assumption held true (approximately), as C_d fluctuated less than 5% from the average value. At α = 0 deg., C_d fluctuated by nearly 20%, with the highest value of C_d occurring at the highest spanwise station.

The 3-D casting followed a similar pattern, with the highest value of C_d also occurring at the highest spanwise station at α = 0 deg. (Fig. 16). Also at this angle of attack, the casting had significantly more fluctuation in C_d than was found in the 2-D simple-geometric simulation, most likely due to the three-dimensional nature of the shape and bubble variation. At α = 4 deg., most of this fluctuation disappeared, and the C_d curve was much flatter than for the α = 0 deg. case. Additionally, C_d decreased slightly at higher spanwise stations, contrary to the trends seen at α = 0 deg. These variations in C_d show the importance of selecting a representative spanwise station at which to measure drag and also that there is a large degree of uncertainty when comparing C_d of various simulations at a single spanwise station.

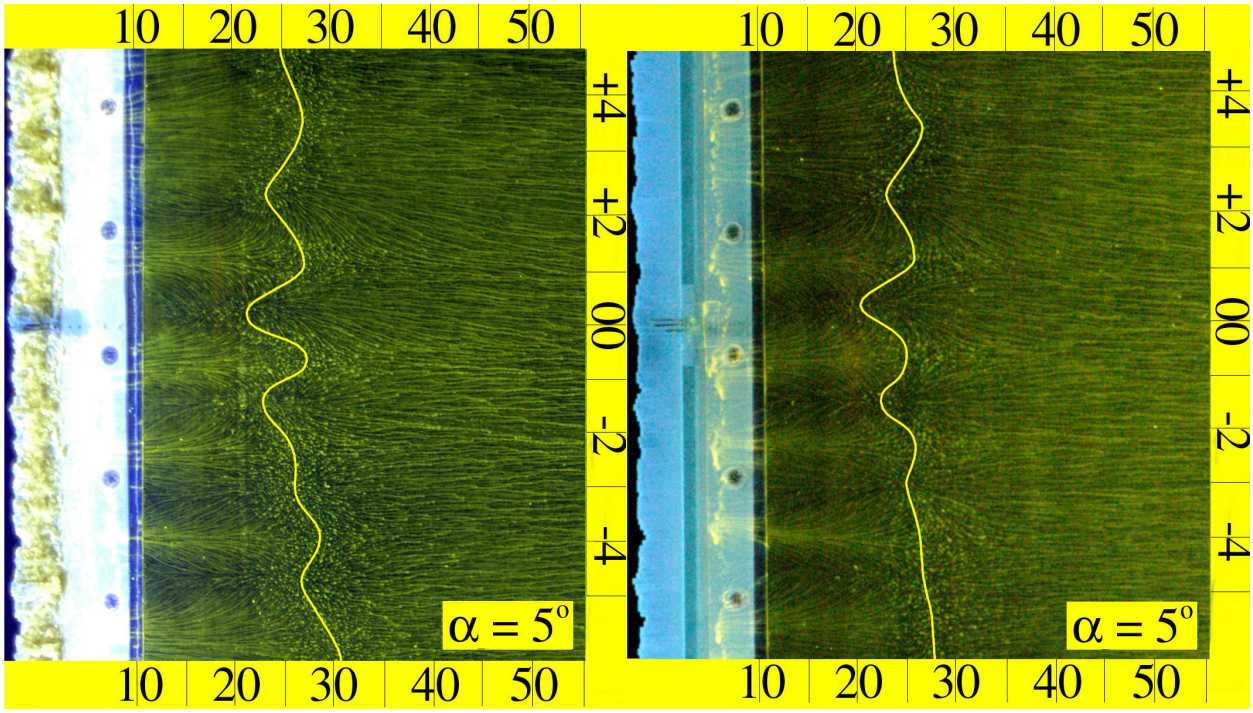

(a) **(b)**

Fig. 13 Comparison of the flowfield behind the (a) 3-D casting and (b) non-periodic simulation at α = 5 deg. and Re = 1.8 million. This image is of the center third of the airfoil model only. The mean separation bubble reattachment line has been highlighted.

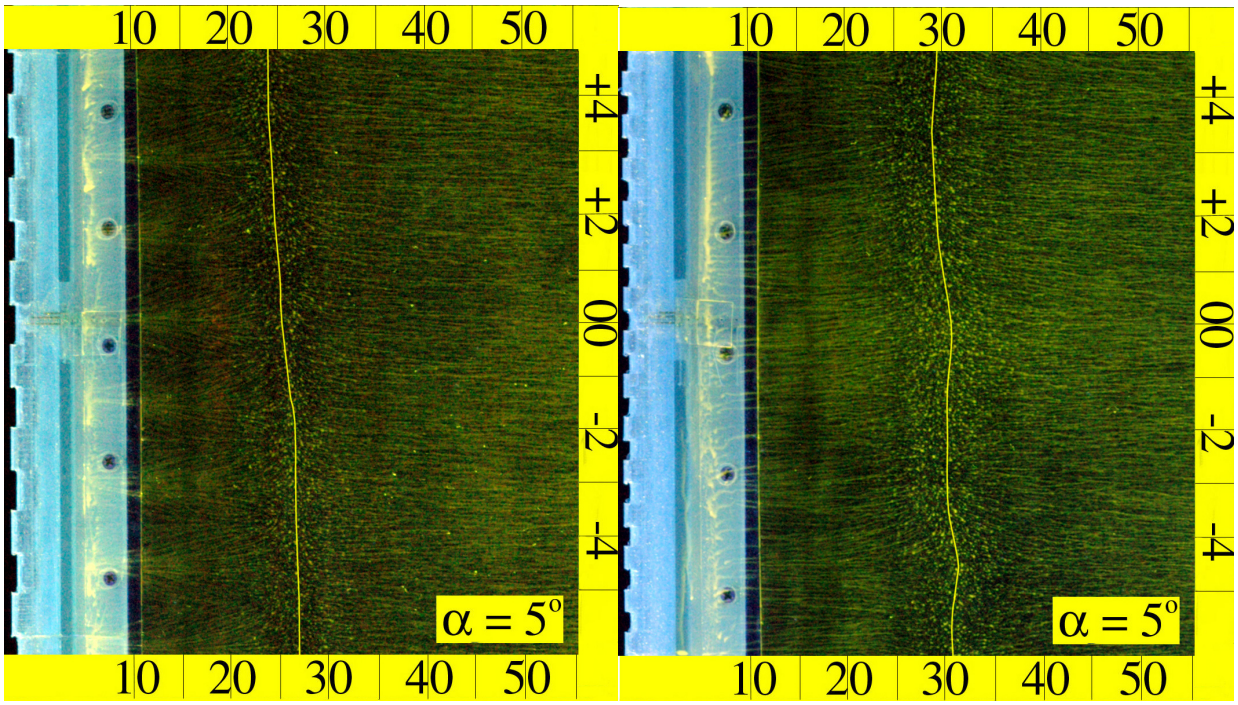

(a) **(b)**

Fig. 14 Fluorescent oil-flow visualization images for the (a) 1.6-inch period and (b) 0.8-inch period simulations at α = 5 deg. and Re = 1.8 million.

A possible explanation for the increased spanwise variation in C_d at α = 0 deg. compared with that at α = 4 deg. is that the separation bubble behind the horn at the higher angle was larger than at the smaller angle. Thus, the separation bubble may have come to dominate the flowfield, damping out the effects of small variations in the horn geometry and helping to smooth the spanwise C_d curve. On the other hand, a similar trend, although not as extreme, was seen for the 2-D simple-geometric simulation, which had no variation in the horn geometry. This would indicate that the spanwise variation in horn-geometry on the casting may not have been the only cause for the relative differences in spanwise variation between the two angles of attack. Further investigation is required to determine other possible sources of these differences.

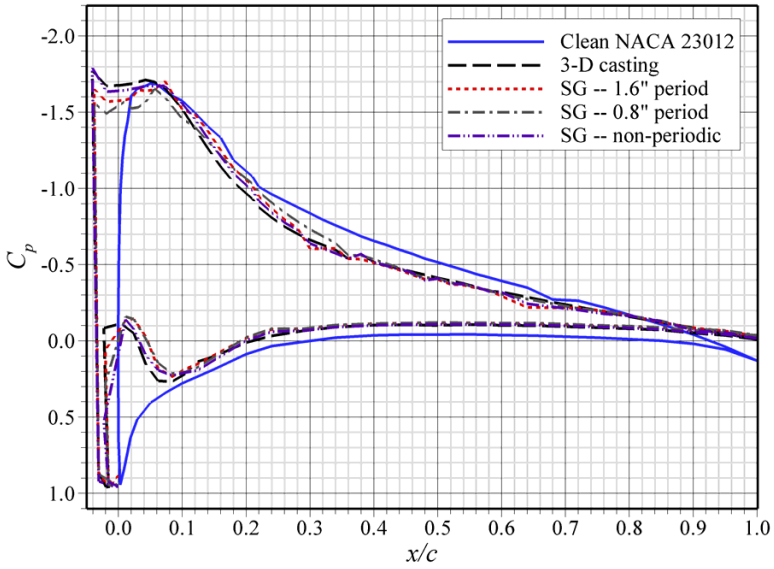

Fig. 15 Comparison of C_p distributions of the 3-D casting and the 3-D simulations at α = 5 deg. and Re = 1.8 million.

The C_d of the 2-D smooth simulation agreed very well with that of the casting at α = 4 deg. at most spanwise stations. At α = 0 deg., the agreement is not as good, as the C_d of the 2-D smooth simulation is below that of the casting at all spanwise stations above z = 1 inch. Since the C_d values shown in Fig. 5b were all taken at z = 3.63 inches, the figure implies that C_d of the 2-D smooth simulation was substantially lower than that of the casting at α = 0 deg. However, it can be seen from Fig. 16 that it actually falls within the range of C_d values measured over the span of the casting. The same is true for the simple-geometric simulation. While it had a C_d that was even less than that of the 2-D smooth simulation at α = 0 deg., its highest value of C_d still fell within the range of C_d measured over the span of the casting.

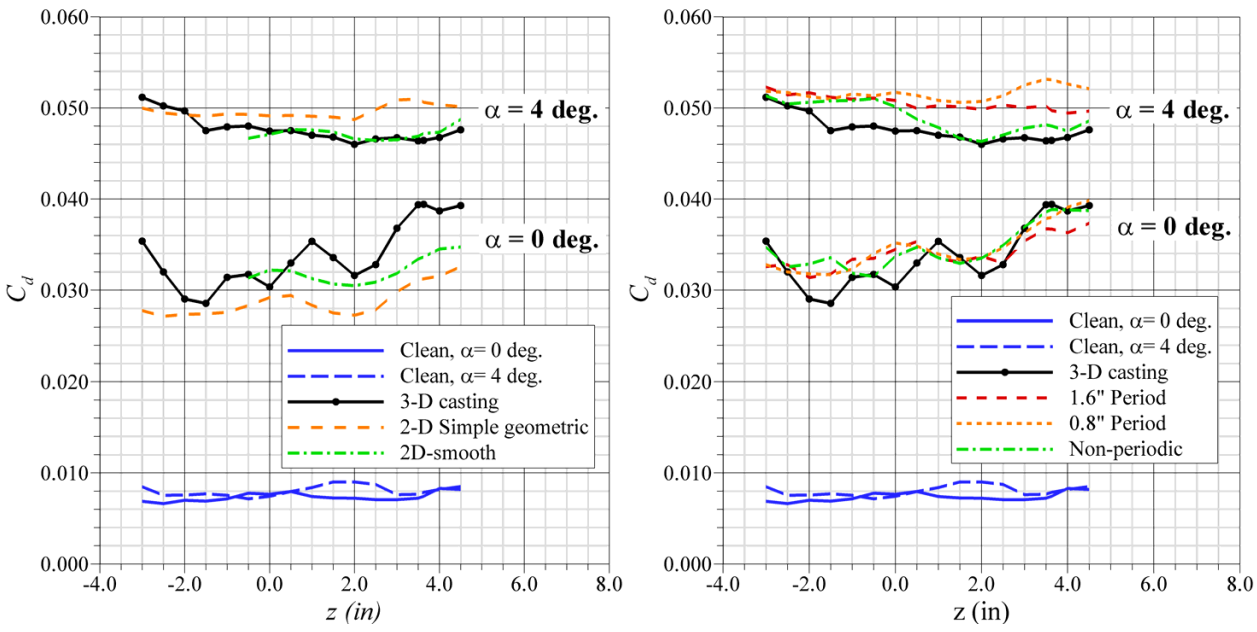

(a) **(b)**

Fig. 16 Spanwise drag comparison of 3-D casting with the (a) 2-D and (b) 3-D simulations.

A comparison between spanwise-drag measurements for each of the horn-ice simulations with spanwise variation is shown in Fig. 16b. At α = 0 deg., the casting showed more fluctuation in C_d than did the other simulations. The periods of the spanwise-drag measurements were similar for each of the simulations, although the phase is shifted. Also, C_d tended to increase at higher spanwise stations, but this was not likely to be caused by spanwise variation of the simulations, since this increase was also present for the 2-D simple-geometric simulation.

The two simple-geometric simulations with periodic spanwise variation had C_d curves which were similar to each other, with the 0.8-inch period simulation having a slightly higher C_d at α = 4 deg. The RMS difference in drag along the span at α = 0 deg. was 0.0023 for the 1.6-inch period simulation and 0.0021 for the 0.8-inch period simulation. The periods of the simulations do not appear to have had a large effect on the spanwise drag measurements, as both periodic simulations have increases in C_d at the same spanwise stations. Also, it can be seen by comparing Fig. 16b with Fig. 16a that the fluctuations which occurred in C_d for the periodic simple-geometric simulations coincided with the fluctuations in C_d for the 2-D simple-geometric simulation, indicating that the fluctuations were not caused by spanwise variation of the simulations. Comparison of these figures also reveals that C_d of the periodic simulations at α = 0 deg. was on average about 15% to 20% higher than that of the 2-D simple-geometric simulation at the same spanwise station. At α = 4 deg., the difference was only a few percent.

Agreement in C_d between the 3-D casting and the non-periodic simple-geometric simulation was slightly better than for the simulations with periodic spanwise variation (especially at α = 4 deg.), with the RMS difference along the span being 0.0021 and 0.0017 for α = 0 deg. and 4 deg., respectively. Despite this, the shape of the spanwise drag curve for the non-periodic simulation was very different from that of the casting. Regions of higher drag on the casting did not correspond well to regions of higher drag on the non-periodic simulation, other than the general trend of increasing C_d at higher spanwise stations. Figure 16b shows that C_d at a spanwise station of 3.63 inches is very similar for the two simulations, which is why the drag polars in Fig. 12b match so closely.

Overall, the non-periodic simple-geometric simulation most accurately represented the C_d of the horn-ice casting. This simulation was also best for simulating the casting $C_{l,max}$, so it is the most representative simulation of the original ice accretion. Unfortunately, detailed measurements of the ice accretion horn height and angle must be made in order to fabricate this type of simulation. For this study, these measurements were made indirectly using a casting. If no casting is constructed, however, the ice accretion must be measured directly, which poses additional challenges. It would be beneficial to create a 2-D smooth simulation instead, which would be much easier to construct. This type of simulation also had a $C_{l,max}$ value similar to the casting. The C_d values were not as close as the non-periodic simple-geometric simulation, but they still fell within the uncertainty in C_d at higher angles of attack due to the widespread spanwise variation in C_d of the casting. This simulation may therefore be sufficient, depending on the accuracy desired. The addition of roughness to this type of simulation must be carefully considered, as it is difficult to gauge the appropriate roughness size to predictably improve the simulation fidelity.

IV. Summary and Conclusions

The objective of this study was to determine the required simulation fidelity to accurately simulate the aerodynamics of a horn-ice accretion. Several different fidelity simulations were constructed to model a horn-ice accretion on a NACA 23012 airfoil, which were a 3-D casting, a 2-D simple-geometric simulation, a 2-D smooth simulation, two simple-geometric simulations with periodic spanwise variation (with periods of 0.8 inches and 1.6 inches), and a simple-geometric simulation which varied the horn height and angle non-periodically every 0.1 inches along the span to match the horn on the casting. Aerodynamic testing and oil-flow visualization were performed in the University of Illinois 3 x 4 ft. subsonic wind tunnel.

The 3-D casting of the horn-ice accretion caused a 55% decrease in $C_{l,max}$ and a 400% increase in $C_{d,min}$ at Re = 1.8 million and M = 0.18. It changed the airfoil stall type from leading-edge stall at α = 14.4 deg. to thin-airfoil stall at α = 7.2 deg. All of the simulations caused the airfoil to exhibit similar behavior, and the effects of each are summarized in Table 2. The farthest left column shows the simulation type and the second column shows the difference in $C_{l,max}$ between the simulation and the casting (with zero being perfect agreement). The third column shows the difference in α_{stall} between the simulation and the casting, and the last column shows the RMS difference in C_d between the simulation and the casting over the range α = -4 deg. to 6 deg.

The 2-D smooth and non-periodic simulations modeled $C_{l,max}$ almost exactly. The next most-accurate simulations were created by adding roughness to the 2-D smooth and simple-geometric simulations. The simulations with periodic spanwise variation both under-estimated $C_{l,max}$ by a larger margin and poorly modeled C_d.

The simulation that most accurately modeled C_d over a wide range of angles of attack was the non-periodic simulation, which had an RMS difference in C_d of only 0.0021 from α = -4 deg. to α = 6 deg. The 2-D simulations under-estimated C_d at low angles of attack and over-estimated it at high angles of attack, resulting in an RMS

difference of 0.0062 for the simple-geometric simulation and 0.0054 for the 2-D smooth simulation. An attempt to improve simulation fidelity was made by adding two sizes of roughness to the 2-D simulations, but the only roughness size to improve the estimate of C_d was not the same as the roughness size on the casting. When the appropriate size roughness was added (k/c = 0.0033), the simulation over-estimated C_d by more than it under-estimated it without roughness. Therefore, based on this test, the appropriate size roughness can not be easily determined without advance knowledge of the accretion aerodynamics. Also, roughness reduced the ability of each simulation to estimate $C_{l,max}$, so it is not recommended at this time that roughness be used to improve simulation fidelity. It is possible that the higher drag of the casting was due to the highly irregular horn geometry, which is why the non-periodic simulation was able to more accurately model C_d while the 2-D simulations with roughness were not.

Table 2 Aerodynamic accuracy of various horn-ice simulations.

Simulation	Simulation $C_{l,max}$ - Casting $C_{l,max}$	Simulation α_{stall} - Casting α_{stall} (deg)	Δ RMS C_d between Simulation and Casting α = -4 to 6 deg.
SG, non-periodic	0.000	0.0	0.0021
2-D smooth	0.001	0.0	0.0054
Simple-geometric	-0.013	0.0	0.0062
2-D smooth + size 35 and 40 microbeads	-0.017	0.0	0.0079
SG + size 35 and 40 microbeads	-0.020	0.0	0.0052
SG, 0.8-inch period	-0.026	0.0	0.0102
SG, 1.6-inch period	-0.051	0.9	0.0070

Significant spanwise variation was observed in the flowfield behind the casting. This variation was not present in the flowfield of either of the 2-D simulations, but was present in the flowfield of the 3-D simulations. In fact, the non-periodic simulation almost exactly reproduced the flowfield of the casting, and was the most accurate simulation. Unfortunately, it is challenging to produce such a simulation, as the accretion horn height and angle must be measured at many locations along the span. This process was simplified in this study because a casting of the accretion was available, but it would be substantially more difficult to make these measurements on the actual accretion.

The improvement in aerodynamic accuracy of the non-periodic simulation may not be sufficient to outweigh the fabrication effort. Instead, a 2-D smooth simulation is recommended for most simulation needs. This type of simulation is relatively simple to construct and accurately modeled $C_{l,max}$. It under-estimated C_d by a small amount at low angles of attack, but was well within the uncertainty of the casting C_d due to spanwise variation.

Acknowledgments

This work was made possible through NASA grant NCC3-1039 from the NASA Glenn Research Center. The authors thank Gene Addy and Sam Lee from NASA Glenn for their valuable support and assistance during the course of this investigation.

References

[1] Bragg, M., Broeren, A., Addy, H., Potapczuk, M., Guffond, D., and Montreuil, E., "Airfoil Ice-Accretion Aerodynamic Simulation," AIAA-2007-0085, *45th Aerospace Sciences Meeting & Exhibit*, Reno, NV, Jan. 2007.

[2] Bragg, M. B., Broeren, A. P., and Blumenthal, L. A., "Iced-Airfoil Aerodynamics," *Progress in Aerospace Sciences*, Vol. 41, 2005, pp. 323-362.

[3] Tani, I., "Low Speed Flows Involving Bubble Separations," *Progress in Aerospace Sciences*, Vol. 5, 1964, pp. 70–103.

[4] McCullough, G.B., and Gault, D.E., "Examples of Three Representative Types of Airfoil-Section Stall at Low Speed," NACA TN-2502, Sep. 1951.

[5] Kim, H.S., and Bragg, M.B., "Effects of Leading-edge Ice Accretion Geometry on Airfoil Aerodynamics," AIAA-99-3150, *17th AIAA Applied Aerodynamics Conference*, Jun. 1999.

[6] Lee, S. "Effects of Supercooled Large Droplet Icing on Airfoil Aerodynamics, Ph. D. Dissertation, University of Illinois at Urbana-Champaign, 2001.

[7] Papadakis, M., Alansatan, S., and Seltmann, M. "Experimental Study of Simulated Ice Shapes on a NACA 0011 Airfoil," AIAA-1999-0096, *37th AIAA Aerospace Sciences Meeting & Exhibit*, Reno, NV, Jan. 1999.

[8] Vickerman, M.B., Choo, Y.K., Schilling, H.W., Baez, M., Braun, D.C., and Cotton, B.J., "Toward an Efficient Icing CFD Process Using an Interactive Software Toolkit – SmaggIce 2-D," AIAA-2002-0380, *40th AIAA Aerospace Sciences Meeting & Exhibit*, Reno, NV, Jan 2002.

[9] Gurbacki, H. M. and Bragg, M.B., "Unsteady Aerodynamic Measurements on an Iced Airfoil," AIAA–2002–0241, *40th AIAA Aerospace Sciences Meeting & Exhibit*, Reno, NV, 2002.

[10] Addy, Jr., H. E. and Chung, J. J., "A Wind Tunnel Study of Icing Effects on a Natural Laminar Flow Airfoil," AIAA–2000–0095, *38th AIAA Aerospace Sciences Meeting & Exhibit*, Reno, NV, Jan. 2000.

[11] Addy, Jr., H. E., Broeren, A. P., Zoeckler, J. G., and Lee, S., "A Wind Tunnel Study of Icing Effects on a Business Jet Airfoil," AIAA–2003–0727, *41st AIAA Aerospace Sciences Meeting & Exhibit*, Reno, NV, Jan. 2003.

[12] Blumenthal, L.A., Busch, G.T., Broeren, A.P., and Bragg, M.B. "Issues in Ice Accretion Simulation on a Subscale Model," AIAA-2006-0262, *44th AIAA Aerospace Sciences Meeting & Exhibit*, Reno, NV, Jan. 2006.

[13] Jacobs, J.J. and Bragg, M.B., "Particle Image Velocimetry Measurements of the Separation Bubble on an Iced Airfoil," AIAA-2006-3646, *24th AIAA Applied Aerodynamics Conference*, San Francisco, CA, Jun. 2006.

[14] Broeren, A.P., "An Experimental Study of Unsteady Flow over Airfoils near Stall," Ph.D. Dissertation, Department of Mechanical Eng., Univ. of Illinois, Urbana, IL, 2000.

[15] Blumenthal, L., "Surface Pressure Measurement on a Three-Dimensional Ice Shape," M.S. Thesis, Univ. of Illinois at Urbana-Champaign, 2005.

[16] Busch, G. T., "Ice Accretion Aerodynamic Simulation on a Subscale Model," M.S. Thesis, Univ. of Illinois at Urbana-Champaign, 2006.

[17] Kline, S. and McClintock, F. A., "Describing Uncertainty in Single-Sample Experiments," *Mechanical Engineering*, Vol. 75, 1953, pp. 3–8.

[18] Coleman, H. W. and W.G. Steel, J., *Experimentation and Uncertainty Analysis for Engineers*, Wiley-Interscience, NY, 1989.

[19] Papadakis, M., Yeong, H., Wong, S., Vargas, M., and Potapczuk, M., "Aerodynamic Performance of a Swept Wing with Ice Accretions," AIAA-2003-0731, *41st AIAA Aerospace Sciences Meeting & Exhibit*, Reno, NV, Jan. 2003.

[20] Wright, W.B., "User Manual for the NASA Glenn Ice Accretion Code LEWICE Version 2.0," NASA CR-1999-209409, Sep. 1999.

[21] Papadakis, M., Gile Laflin, B. E., Youssef, G. M., and Ratvasky, T. P., "Aerodynamic Scaling Experiments with Simulated Ice Accretions," AIAA-2001-0833, *39th AIAA Aerospace Sciences Meeting & Exhibit*, Reno, NV, Jan. 2001.